J Therm Anal Calorim (2014) 116:625–632
DOI 10.1007/s10973-014-3759-6

Thermal behaviour of natural and synthetic iron precipitates from mine drainage

P. Pulišová · B. Máša · E. Michalková · E. Večerníková · M. Maříková · P. Bezdička · N. Murafa · J. Šubrt

Received: 30 September 2013 / Accepted: 14 March 2014 / Published online: 10 April 2014

Abstract TG–DTA, MS detections and XRD were used to characterize thermal behaviour of iron precipitates from acid mine drainage prepared by precipitation with urea and natural iron precipitates sampled from sludge bed (settling pit *Sedem žien* and old abandoned adit *Hodruša*, mining area Banská Štiavnica, Slovakia). The high-resolution transmission electron microscopy and scanning electron microscopy (SEM) techniques were used to characterize the surface microstructure and shape of the synthesized and sampled iron precipitates. The SEM micrographs of the iron precipitates (natural and precipitated with urea) show that the samples had formed into agglomerates, probably due to attractive forces of quite large surface area. During heating of the all samples up to 200 °C, physically adsorbed water was removed. On further heating in the range from 250 to 350 °C in natural iron precipitates, the less stable forms (goethite, ferrihydrite, and schwertmannite) transform to more stable forms like hematite. In case of synthetic samples, the transformation runs in two steps: first in the range from 250 to 350 °C, and second in the range from 600 to 750 °C.

Keywords Thermogravimetry · Differential thermal analysis · X-ray diffraction analysis · Acid mine drainage · Iron precipitates · Precipitation with urea

P. Pulišová (✉) · E. Večerníková · M. Maříková · P. Bezdička · N. Murafa · J. Šubrt
Institute of Inorganic Chemistry of the AS CR, v.v.i, Husinec-Řež č.p. 1001, 250 68 Husinec-Řež, Czech Republic
e-mail: pulisovap@yahoo.com

B. Máša · E. Michalková
Faculty of Ecology and Environmental Sciences, Technical University in Zvolen, T.G. Masaryka 2117/24, 960 53 Zvolen, Slovak Republic

Introduction

Sulphide minerals (like pyrite, pyrholite, marcasite, etc.), which can be found in old deposits after coal-, and gold minings, and in polymetallic ores, are transformed to the acid mine drainage (AMD). This is due to their modifications being liable to microbiological–chemical biodegradation by action of chemolithotrophic bacteria, namely genera Acidithiobacillus and Leptospirillum, under aerobic conditions (air and water) [1–4]. AMD is characterized by low pH value (pH $\leq$ 3), various dissolved metals (Fe, Al, Zn, Pb, etc.) and high concentration of SO_4^{2-}. The precipitation of ferric compounds from AMD is a process of formation of different solid phases at different pH values and sulphate concentrations [4–7].

Natural iron precipitates are formed from AMD from solid phases of ferric oxyhydroxides like ferrihydrite $Fe_5HO_8{\cdot}4H_2O$, schwertmannite $Fe_8O_8(OH)_6SO_4$, jarosite $(NaKH_3O)^+Fe_3(SO_4)_2(OH)_6$, goethite α-FeOOH or a mixture containing all three species [6–9]. They are frequently a by-product of metabolic processes in microorganisms containing iron (Fe^{2+}) as an energy source [10]. The mixing and diluting of AMD with a fresh water stream, in drainage channels or in other places where mine water discharges, facilitate the formation of iron precipitates with various compositions [11]. Some of the resulting iron oxides are susceptible to external conditions (temperature, atmospheric effluence, etc.), and when these conditions are present, transformation of less stable oxides to the more stable forms takes place. Due to a different genesis, the iron precipitates vary in size and relatively high ratio of water molecules [12–14].

Knowledge of the thermal behaviour of iron precipitates has importance in final treatment of produced iron oxide materials and also in industrial application of products.

Another possible application of iron precipitates is the detoxification of some pollutants based on the high surface area and the high reactivity of materials prepared by the homogeneous precipitation method of various metal salts with urea.

In this study, we used simple methods to treat natural iron precipitates (washing with de-ionized water, drying at room temperature) and to treat AMD using homogenous precipitation by urea to obtain synthetic iron precipitates [15]. By hydrolysis of AMD in the temperature range from 60 to 95 °C with urea, it is possible to prepare easily filterable relative pure ferric precipitates. Depending on the conditions of homogeneous precipitation, the resulting precipitates consist of various amorphous or crystalline phase (jarosite, schwertmannite, goethite, ferrihydrite, etc.). The physical properties of such treated natural iron precipitates and of prepared synthetic iron precipitates were investigated. High specific surface areas of natural and synthetic iron precipitates were examined. The iron precipitates can be used further for sorption and removal of phosphates, arsenic, chlorine hydrocarbons, and organic dyes from contaminated waste waters [16]. It was also examined that during heat treatment, the less stable forms of ferrihydrite, schwertmannite, and goethite transform to the more stable form—hematite.

Experimental

Preparation of samples

Natural iron precipitates were sampled from abandoned mine adits and settling pits from the mining area, Banská Štiavnica located near Hodruša, Slovakia. The natural iron precipitates were washed by de-ionized water and dried at room temperature. Synthetic iron precipitates were prepared by precipitation, using urea of AMD collected from the spoil dump of pyritized quartzite Šobov (Banská Štiavnica). The precipitation step was in the temperature range from 60 to 95 °C. The reaction was finished when molar ratio of urea to iron was 10:1, and the pH value was approx. 3.5 (more than 95 % of iron were selectively dropped out from AMD). The synthetic iron precipitate was then filtered and washed with de-ionized water. The last step of procedure consists of drying the precipitate at room temperature. Urea used for precipitation of AMD was of analytical-grade purity chemicals provided by Sigma-Aldrich, Germany.

Methods of samples characterization

Thermogravimetry (TG) and differential thermal analysis (DTA) and evolved gas analysis/mass spectrometry (EGA/MS) measurements were carried out by heating the iron precipitates in air (synthetic 30 mL min^{-1}) by using SETARAM SETSYS Evolution-16-MS equipment. Gaseous products were analysed in the MID mode as Intensity (*A*) of individual selected fragments. The mass of each sample measured was 20 mg and the heating rate was 10 °C min^{-1} (from 20 to 1,100 °C).

Diffraction patterns were collected using a PANalytical X′Pert PRO diffractometer, equipped with a conventional X-ray tube ($Co_{K\alpha}$ radiation, 40 kV, 30 mA, line focus), and a multichannel detector X'Celerator with an anti-scatter shield. We used conventional Bragg–Brentano geometry with 0.04 rad Soller slit, 0.5° divergence slit, 1° anti-scatter slit, and 15-mm mask in the incident beam, 5.5-mm anti-scatter slit, 0.04 rad Soller slit, and Fe beta-filter in the diffracted beam. In the case of collected or synthesized samples, we used a side-loaded sample holder, and the X-ray patterns were measured in the range from 10° to 95° 2Θ with steps of 0.0167° and 1,050 s counting per step. Samples after thermal analysis were spread on silicon zero-background sample holder, and X-ray patterns were measured in the range of 10° to 95° 2Θ with steps of 0.0167° and 250 s counting per step. XRD patterns were not pretreated before interpretation as no background correction was needed. Qualitative analysis was performed using the HighScorePlus software package (PANalytical, The Netherlands, version 3.0e), Diffrac-Plus software package (Bruker AXS, Germany, version 8.0) and JCPDS PDF-2 database (release 2004).

To characterize the particle size and structural morphology of the collected and synthesized iron precipitates, a high-resolution transmission electron microscopy (HRTEM, Type JEM-3010, JEOL) at 300 kV accelerating voltage, equipped with EDX (Energy Dispersive X-ray) and the Philips XL 30 CP microscope equipped with EDX, Robinson, SE (Secondary Electron) and BSE (Back-Scattered Electron) detectors were used. For the observations by SEM in SE electrons, the samples were coated with thin conductive Au–10 % Pd alloy layer.

Specific surface area was determined by the B.E.T. (Brunauer–Emmett–Teller) method [17] from nitrogen adsorption–desorption isotherm acquired at liquid-nitrogen temperature using a NOVA 4200e instrument. A 12-h outgas at 80 °C was used before the measurement.

Results and discussion

Figures 1 and 2 depict the results of TG–DTA and the results of EGA/mass spectrometry (MS) detection of the gases evolved during air heating. Simultaneous measurements of thermogravimetric analysis (TG) and differential thermal analysis (DTA) were carried out at flow

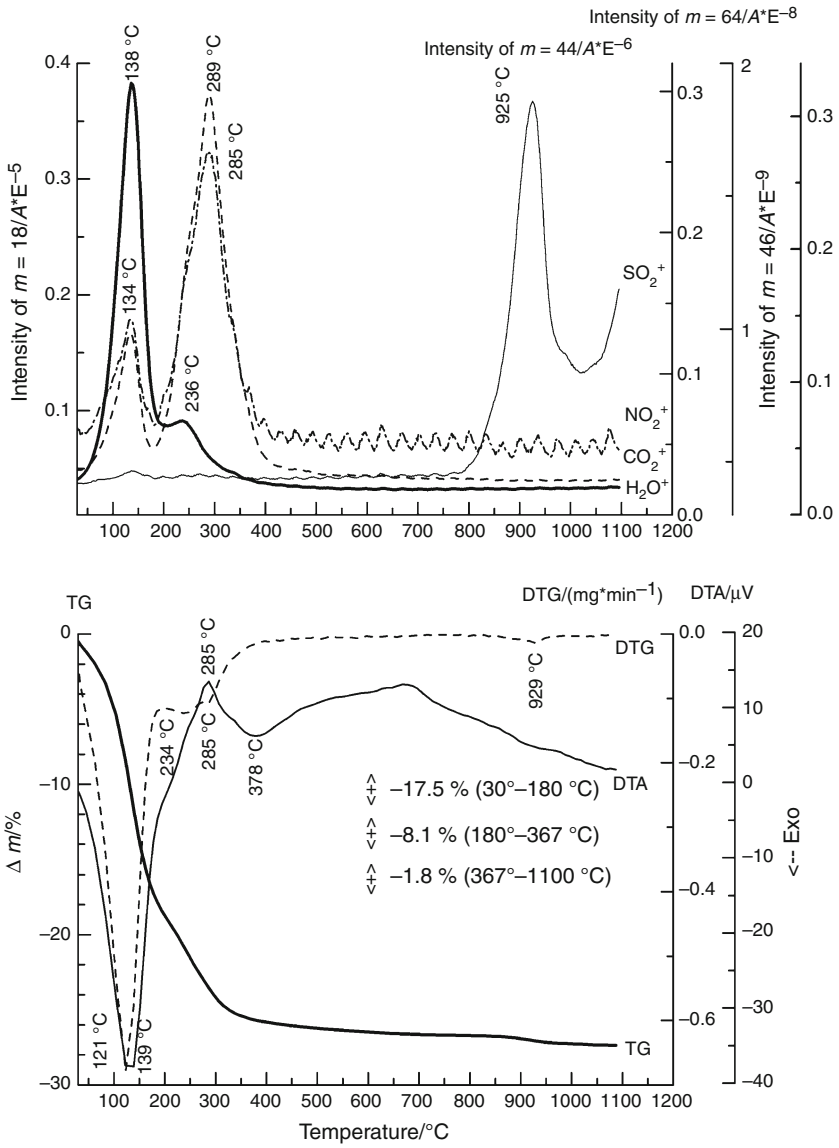

Fig. 1 EGA/MS, TG and DTA results of natural iron precipitate (sampled in-settling pit locality Banská Štiavnica, Slovakia) measured on heating in air

rates from 20 to 1,100 °C in 30 mL min^{-1} of air at the heating rate of 10 °C min^{-1}. Gaseous products were analysed in the MID mode as intensity (A) of individual selected fragments.

Figure 1 depicts the results of thermal analysis of the natural iron precipitate compared with results of the synthetic iron precipitate (Fig. 2). From the TG–DTA curve (Fig. 1) up to 400 °C indicating two consecutive steps of the mass loss 25.6 %, which could be attributed to the release of physically adsorbed water, dehydroxylation reactions, and release of NO_x and CO_2, we can see these in the form of broad endothermic peak on DTA curve. The endothermic peak at 139 °C indicating the release of CO_2 and the exothermic peak at 289 °C occur due to the burning of carbonaceous material resulting in the formation of CO_2. Exothermic effect around 300 °C is often observed during the transformation of less stable ferrihydrite, goethite and schwertmannite to more thermally and chemically stable hematite [18, 19], which is confirmed by XRD measurements. The dehydroxylation reaction that occurs on heating goethite in air has usually been observed as an endothermic peak in the temperature range from 250 to 400 °C, depending on the particle size and crystallinity of the tested samples. Release of SO_2 is observable from 811 °C to max. 925 °C with the mass loss of 1.8 %. An exotherm/endotherm pair in the range from 400 to 650 °C can be attributed to the formation of $Fe_2(SO_4)_3$ followed by its decomposition to hematite and SO_3, which can be compared with data observed by the Cornell et al. [18].

Figure 2 depicts the results of thermal analysis of the synthetic iron precipitate prepared by precipitation with urea. The TG–DTA curve up to 500 °C is characterized by two consecutive steps of the mass loss 22.6 %, which could be also attributed to the release of physically adsorbed

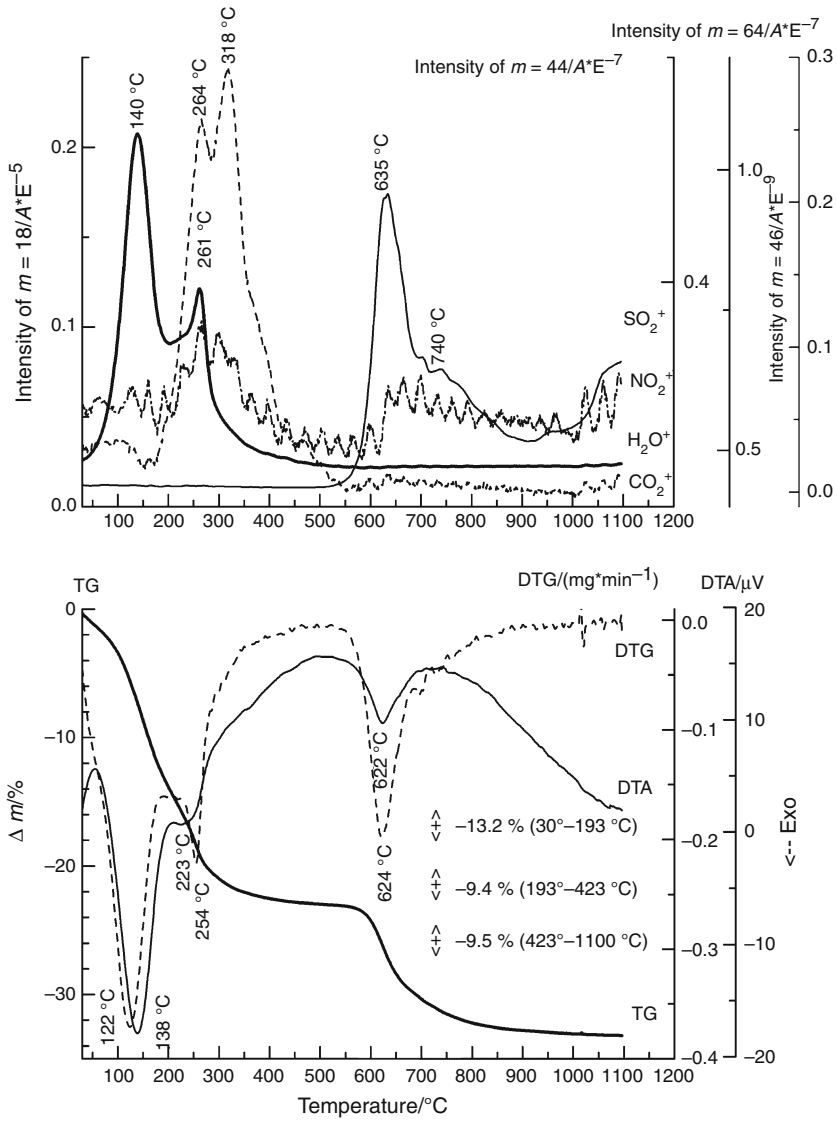

Fig. 2 EGA/MS, TG and DTA results of synthetic iron precipitate measured on heating in air

water, dehydroxylation reactions and release of NO_x and CO_2. We can see endothermic double peaks at 138 and 223 °C on the DTA curve; this corresponds to the loss of adsorbed water and dehydroxylation reactions. Burning of carbonaceous material starts at approx. 200 °C with two maxima on MID_CO_2 curve (264 and 318 °C) if compared with the natural iron precipitate (Fig. 1; 289 °C) connected with broad exothermic effect in the range from 250 to 500 °C. Release of SO_2 that is observable from 550 °C to max. 800 °C indicates the mass loss of 9.5 %. This process is shifted to lower temperature (endothermic effect at 622 °C on DTA curve) in comparison with natural iron precipitate (Fig. 1; 925 °C). The transformation of goethite and schwertmannite to stable hematite is passing over 300 °C [20]. Goethite proceeds directly to hematite without any intermediate phase. The transformation temperature usually depends on the crystallinity. For example, as the crystallinity of goethite improved, the endothermic (DTA) peak temperature shifted from 260 to 320 °C. In addition, a double peak which is attributed to a two-phase transition of well-crystalline goethite to hematite developed. The double dehydroxylation peak has also been associated with high surface area samples, excess surface water and the water vapour pressure [18].

Figure 3 depicts the results of TG–DTA and the results of EGA/mass spectrometry (MS) detection of the gases evolved during air heating. The DTA curve of the another natural iron precipitate from location Hodruša (Slovakia) shows on heating air endothermic peaks at 127 and 268 °C due to the release of physically adsorbed water. The TG–DTA curve up to 450 °C indicating two consecutive steps of the mass loss 27.7 % could be attributed to the release of water, NO_x and CO_2. The exothermic peak at 316 °C occurs due to the burning of CO_2. Continuing in heating from 567 °C to maximum 663 °C indicates the mass loss of 5.4 %, which is attributed to the release of SO_2.

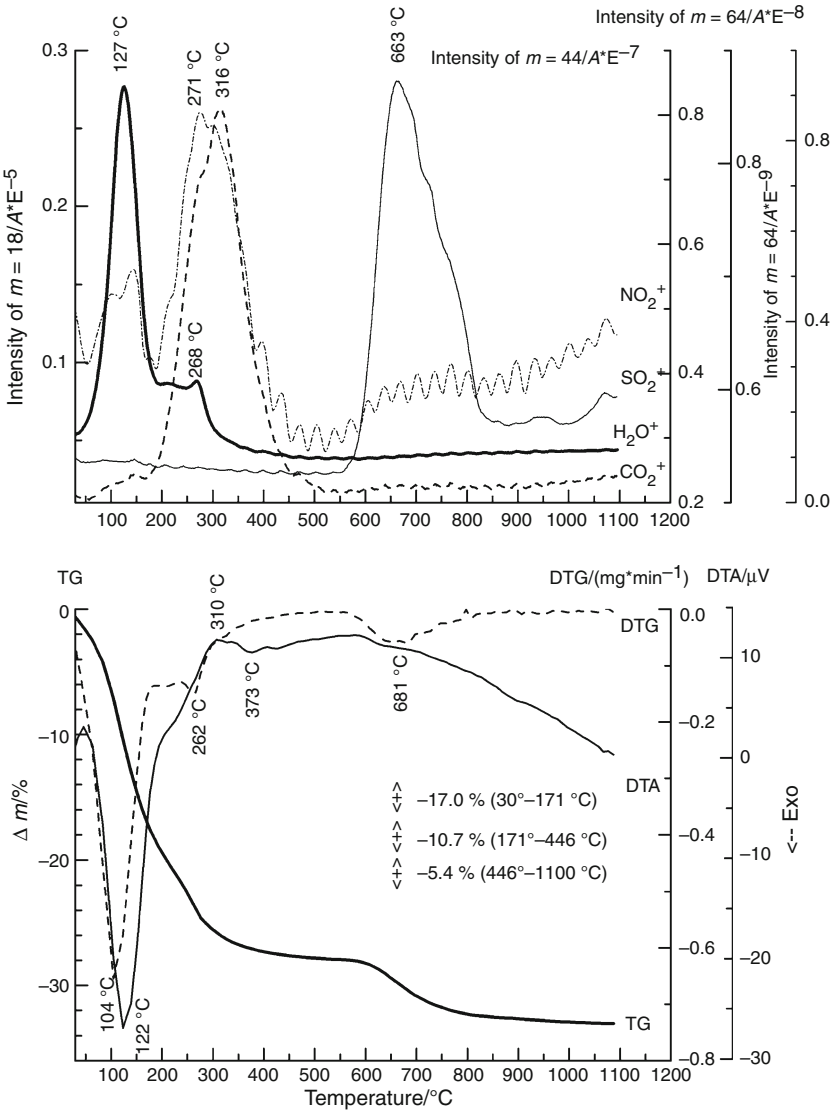

Fig. 3 EGA/MS, TG and DTA results of natural iron precipitate sampled in old adit location, Hodruša, Slovakia measured on heating in air

Powder X-ray diffraction (XRD) was used for determining the phase composition of the collected and synthesized samples. Weakly crystalline goethite was observed in natural sample (location Banská Štiavnica, Slovakia, Fig. 4) collected in mixture with ferrihydrite, goethite, and schwertmannite. Quartz was also identified as a minor phase, probably as a result of contamination during sampling of the natural environment. Quartz particles were partially covered with fine precipitate and could not be separated by a sieving procedure. The presence of quartz was also confirmed by SEM/EDS analysis.

In the case of synthetic iron precipitate (Fig. 5) obtained at laboratory recovery from typical AMD by homogenous precipitation using urea, the schwertmannite with goethite was observed, and the process of their formation is probably affected by the pH value (pH 2–3) [7].

Transformation, after heating in air, to more stable hematite from less stable goethite, ferrihydrite, and schwertmannite in natural iron precipitate from the settling pit locality of Banská Štiavnica (Fig. 6) is confirmed by both the DTA and XRD measurements. Hematite is, in this case, accompanied by traces of quartz and cristobalite. Quartz has already been identified in the collected sample. The presence of cristobalite demonstrates that collected sample should contain some amorphous natural silica.

The same transformation takes place in the case of synthetic iron precipitate (Fig. 7). Less stable mixture of goethite and schwertmannite transforms to more stable hematite. Traces of cristobalite were identified also in this sample after TA. This is probably due to the use of natural water (taken from the pit) which could also be contaminated by amorphous silica.

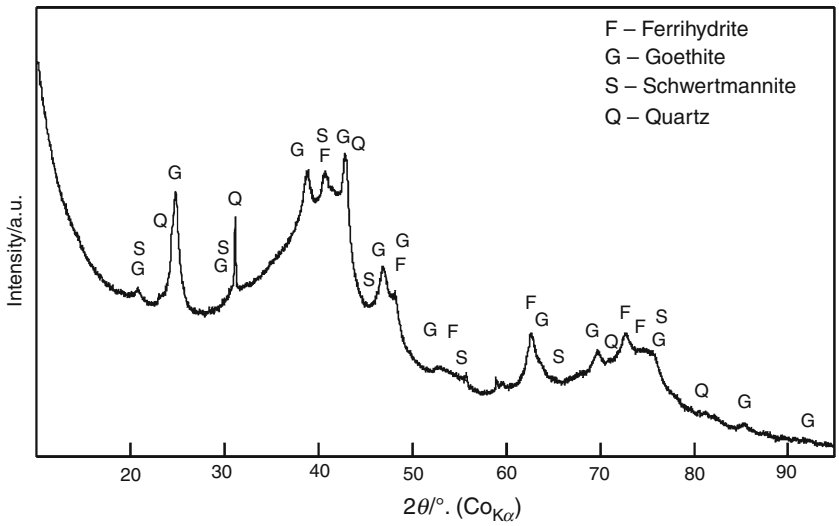

Fig. 4 Powder X-ray pattern of natural iron precipitate from settling pit locality, Banská Štiavnica, Slovakia

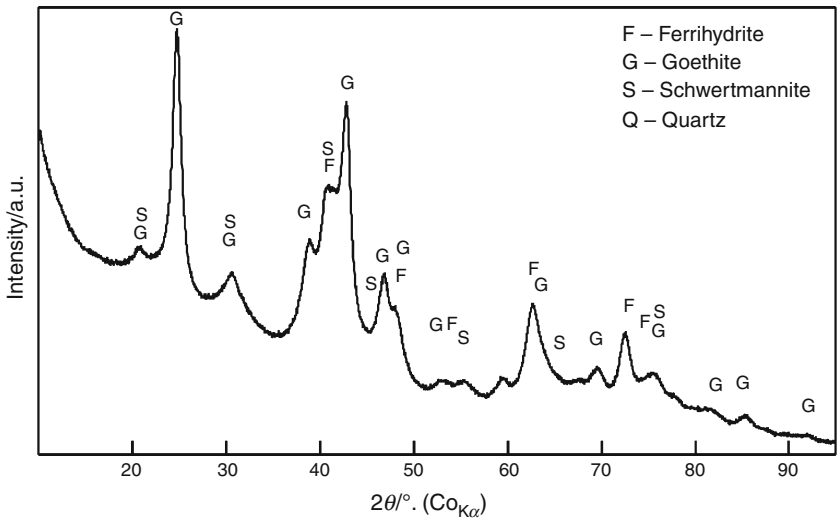

Fig. 5 Powder X-ray pattern of synthetic iron precipitate

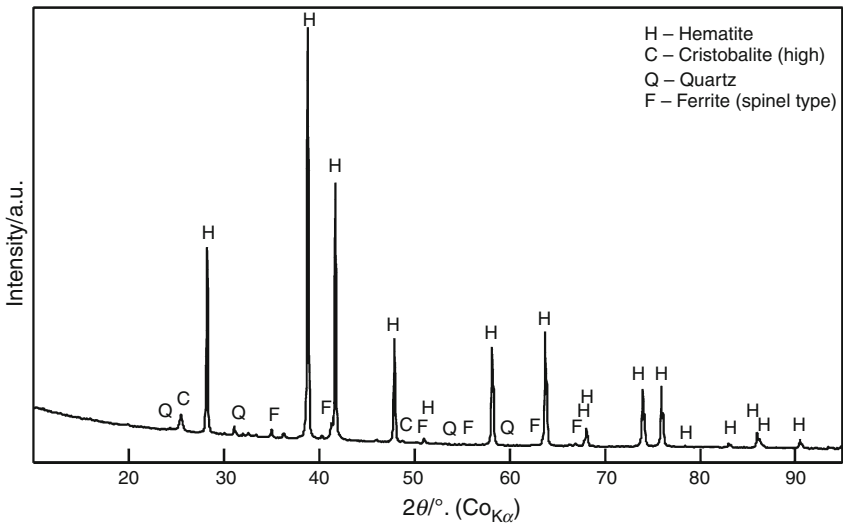

Fig. 6 Powder X-ray pattern of natural iron precipitate after TA

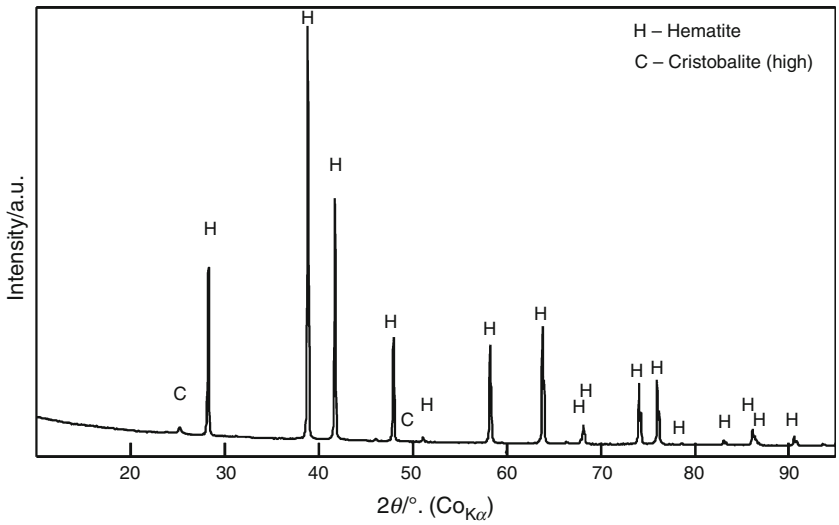

Fig. 7 Powder X-ray pattern of synthetic iron precipitate after TA

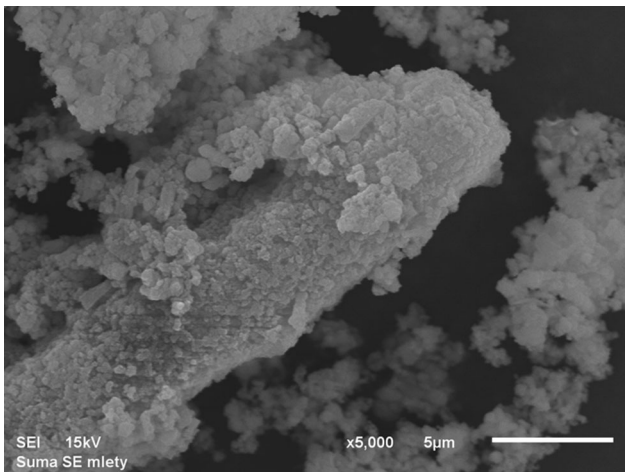

Fig. 8 SEM micrograph of natural iron precipitate

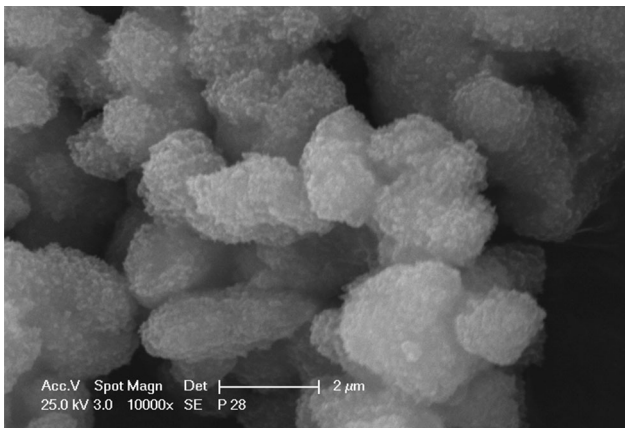

Fig. 9 SEM micrograph of synthetic iron precipitate

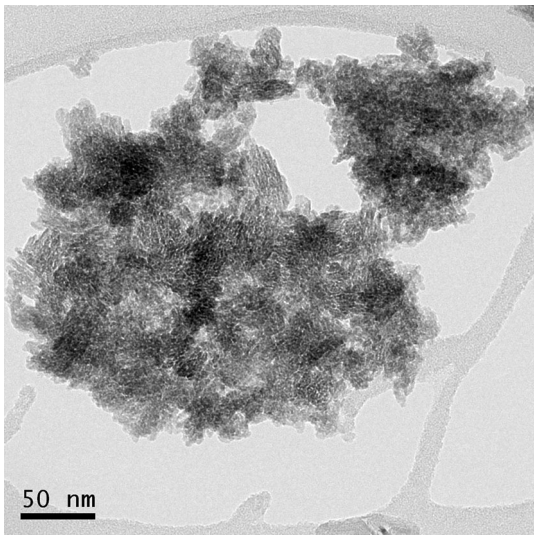

Fig. 10 TEM micrograph of natural iron precipitate

Micrographs from scanning electron microscope and high-resolution transmission electron microscope of natural iron precipitate (Figs. 8, 10) and synthetic iron precipitate (Figs. 9, 11) confirm that the precipitates have agglomerated in few µm (ca. tenths of µm)-sized aggregates.

The specific surface area of natural iron precipitate (settling pit Banská Štiavnica) was 257.7 m^2/g and that of synthetic iron precipitate was 75.7 m^2/g, which is lower in comparison with that of the natural iron precipitate. It corresponds with micrographs from scanning electron microscope (Figs. 8, 9) and with micrographs from high-resolution transmission electron microscope (Figs. 10, 11). The samples have quite high specific surface area, and they

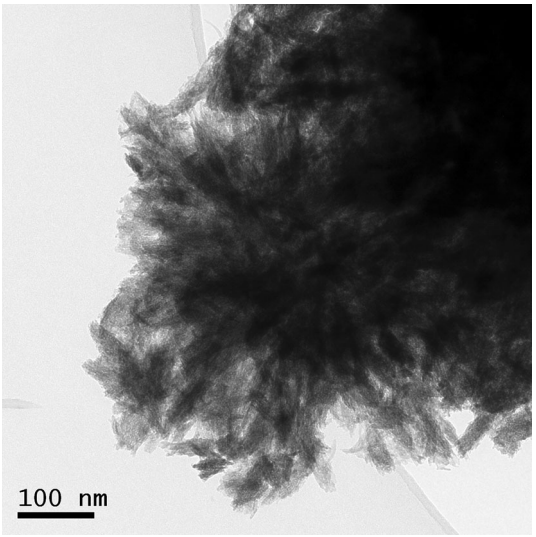

Fig. 11 TEM micrograph of synthetic iron precipitate

could be inexpensive and efficient adsorbents for removal of select pollutants from water environments.

Conclusions

The TG, DTA and EGA/MS detection analyses were used for the characterization of thermal behaviour of iron precipitates. The release of carbonaceous material is shifted to higher temperature (318 °C) in the case of synthetic sample compared with the natural sample (289 °C). In the case of synthetic sample, the transformation runs in two steps: the first in the range from 250 to 350 °C, and the second in the range from 550 to 750 °C. A double peak which is attributed to a two-phase transition of well-crystalline goethite to hematite could be associated with high surface area samples, excess surface water and the water vapor pressure. Powder X-ray diffraction analysis confirmed that, in both cases, the less stable goethite, ferrihydrite and schwertmannite in the natural samples and goethite and schwertmannite in the synthetic samples were transformed after heating in air to more stable hematite. From electron microscopy, it is visible that both natural and synthetic samples have agglomerated into aggregates around tenths of μm. Potentially, such materials can be effectively used for both sorption and removal of phosphates, arsenic, chlorine hydrocarbons and organic dyes from contaminated waste waters or others like pigments.

Acknowledgements This work was supported by the Slovak-Czech Intergovernmental Scientific-Technical Cooperation (APVV SK-CZ-0139-11), by the Ministry of Education, Youth and Sports of the Czech Republic (Project No. 7AMB12SK155).

References

1. Cravotta CA III. Dissolved metals and associated constituents in abandoned coal-mine discharges, Pennsylvania, USA. Part 2: geochemical controls on constituent concentrations. Appl Geochem. 2008;23(2):203–26.
2. Malmström ME, Gleisner M, Herbert RB. Element discharge from pyritic mine tailings at limited oxygen availability in column experiments. Appl Geochem. 2006;21(1):184–202.
3. Druschel GK, Baker BJ, Gihring TM, Banfield JF. Acid mine drainage biogeochemistry at Iron Mountain, California. Geochem Trans. 2004;5(2):13–32.
4. Sánchez Espana J, López Pamo E, Santofimia E, Aduvire O, Reyes J, Barettino D. Acid mine drainage in the Iberian Pyrite Belt (Odiel river watershed, Huelva, SW Spain): geochemistry, mineralogy and environmental implications. Appl Geochem. 2005;20(7):1320–56.
5. Filip J, Zboril R, Schneeweiss O, Zeman J, Cernik M, Kvapil P, et al. Environmental applications of chemically pure natural ferrihydrite. Environ Sci Technol. 2007;41(12):4367–74.
6. Bigham JM, Schwertmann U, Traina SJ, Winland RL, Wolf M. Schwertmannite and the chemical modeling of iron in acid sulfate waters. Geochim Cosmochim Acta. 1996;60(12):2111–21.
7. Hammarstrom JM, Seal Ii RR, Meier AL, Kornfeld JM. Secondary sulfate minerals associated with acid drainage in the eastern US: recycling of metals and acidity in surficial environments. Chem Geol. 2005;215:407–31.
8. Bigham JM, Carlson L, Murad E. Schwertmannite, a new iron oxyhydroxy-sulphate from Pyhasalmi, Finland, and other localities. Mineral Mag. 1994;58:641–8.
9. Schwertmann U, Bigham JM, Murad E. The first occurrence of schwertmannite in a natural stream environment. Eur J Mineral. 1995;7(3):547–52.
10. Kim JJ, Kim SJ, Lee SS. Gallionella Ferruginea in ochreous precipitates from acid mine drainage in Donghae coal mine area, Korea. Geosci J. 2003;7(4):289–92.
11. Kumpulainen S, Carlson L, Raisanen M-L. Seasonal variations of ochreous precipitates in mine effluents in Finland. Appl Geochem. 2007;22(4):760–77.
12. Che Y, Huang W, Liu D, Chen J, Sun Z. Micro-goethite in percolated water from Fushui Reservoir in Hubei Province, China. Mater Sci Eng. 2006;26(4):606–9.
13. Peretyazhko T, Zachara JM, Boily JF, Xia Y, Gassman PL, Arey BW, et al. Mineralogical transformations controlling acid mine drainage chemistry. Chem Geol. 2009;262:169–78.
14. Gagliano WB, Brill MR, Bigham JM, Jones FS, Traina SJ. Chemistry and mineralogy of ochreous sediments in a constructed mine drainage wetland. Geochim Cosmochim Acta. 2004;68(9):2119–28.
15. Šubrt J, Michalková E, Boháček J, Lukáč J, Gánovská Z, Máša B. Uniform particles formed by hydrolysis of acid mine drainage with urea. Hydrometallurgy. 2011;106(1–2):12–8.
16. Ko M-S, Kim J-Y, Lee J-S, Ko J-I, Kim K-W. Arsenic immobilization in water and soil using acid mine drainage sludge. Appl Geochem. 2013;35:1–6.
17. Brunauer S, Emmet PH, Teller E. Adsorption of gases in multimolecular layers. J Am Chem Soc. 1938;60:309–19.
18. Cornell RM, Schwertmann U. The iron oxides: structure, properties, reactions, occurences and uses. Weiheim: Wiley; 2003.
19. Alcolea A, Ibarra I, Caparrós A, Rodríguez R. Study of the MS response by TG–MS in an acid mine drainage efflorescence. J Therm Anal Calorim. 2010;101(3):1161–5.
20. Gialanella S, Girardi F, Ischia G, Lonardelli I, Mattarelli M, Montagna M. On the goethite to hematite phase transformation. J Therm Anal Calorim. 2010;102:867–73.